Biophysical Chemistry 3 (1975) 249–254

EXCHANGE RATES OF PYRIDINE ON FERRO- AND FERRIPROTOPORPHYRIN (IX) DIMETHYLESTER IN CHLOROFORM

E. von GOLDAMMER and H. ZORN

Institut für Biophysik und Physikalische Biochemie, Fachbereich Biologie, Universität Regensburg, Universitätsstr. 31, D-84 Regensburg, Fed. Rep. of Germany

Received 19 November 1974

Nuclear magnetic resonance line-widths data have been used to determine the rate of solvent exchange from the first coordination sphere of ferro- and ferriprotoporphyrin(IX) dimethylester (Fe–PPD) in pyridine/chloroform. The average values of kinetic parameters for pyridine (PY) exchange indicate an SN2 mechanism for Fe(III)–PPD ($\Delta H^{\neq} = 36$ kJ·mol^{-1}; $\Delta S^{\neq} = -53$ J·mol^{-1}K^{-1}; $\tau_M(298\ K) = 0.07$ msec) and an SN1 mechanism for Fe(II)–PPD ($\Delta H^{\neq} = 67$ kJ·mol^{-1}; $\Delta S^{\neq} = 42$ J·mol^{-1}K^{-1}; $\tau_M(298\ K) = 0.06$ msec). Parallel to the accelerated ligand exchange rate at rising temperatures a redistribution of the electrons causing a transition of the metal porphyrin from the low-spin state to the high-spin state is observed. Enthalpy and entropy of the thermodynamic equilibrium between low- and high-spin Fe–PPD have been determined from experimental values of the average magnetic moment. A mean lifetime of low-spin Fe(III)–PPD was estimated from line-widths changes ($\tau_{L\to H}(298\ K) \approx 20$ msec) and the corresponding activation parameters have been obtained ($\Delta H^{\neq}_{L\to H}(298\ K) = 26$ kJ·mol^{-1}; $\Delta S^{\neq}_{L\to H}(298\ K) = -125$ J·mol^{-1}K^{-1}).

1. Introduction

The biological function of metal porphyrins acting as prosthetic groups in many proteins, rests largely upon their ability to exchange ligands coordinated to the metal ion in the axial positions [1]. Nuclear magnetic resonance (NMR) spectroscopy has proved most useful in studying details of electronic and molecular structure of paramagnetic metal complexes [2] and is particularly suited for measuring the kinetic and thermodynamic parameters of the exchange reaction between coordinated and non-coordinated ligands. Although this method has been utilized most extensively with other systems, only few results on metal porphyrins have been reported [3–5]. The resulting data may serve to understand the essential features of iron–porphyrin complexes in biological systems in more detail.

The work presented here, deals with the bis-pyridine complexes of ferro- and ferriprotoporphyrin (IX) dimethylester (Fe(II)–Fe(III)–PPD) in deutero-chloroform, for which NMR signal assignment and chemical-shift measurements already have been reported [6,7].

2. Experimental

A Varian XL-100-15 high-resolution spectrometer operating at 100 MHz has been used for ^{1}H-NMR measurements. The temperature was controlled by a stream of precooled nitrogen and was measured with a calibrated thermocouple in the effluent gas stream. Temperature accuracy was estimated to be ± 1 K. Reproducibility of linewidths (at half height) and chemical shifts was ± 2 Hz. Magnetic susceptibilities were measured as described elsewhere [8,9]. Tetramethylsilane (TMS) was chosen as an inert marker for ^{1}H-NMR susceptibility and shift measurements. All chemical shifts reported here are taken against TMS as internal standard.

The following materials have been used: pyridine and deutero-chloroform (99.8 at% deuterium) of spectroscopic grade (Merck, Darmstadt). Fe(III)–, and Fe(II)–PPD were synthesized as described in the literature [10].

3. Results and discussion

The spin–spin relaxation rates $1/T_2$, derived from

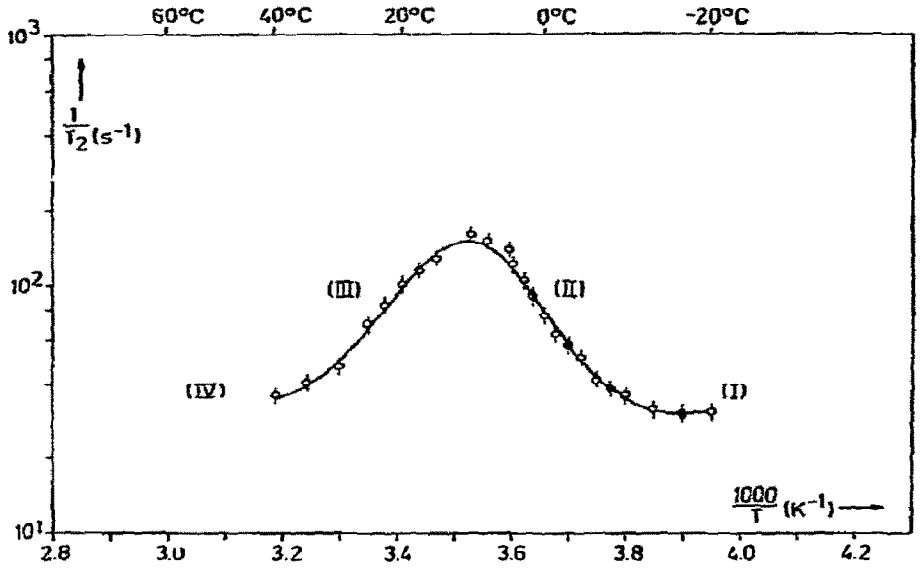

Fig. 1. Spin–spin relaxation rate of the α protons of bulk phase pyridine in solutions of Fe(II)–PPD in $C_5H_5N/CDCl_3$ at various temperatures ($C_M = 2.5 \times 10^{-5}$ m; $C_A = 3.3 \times 10^{-4}$ m; $C_{CDCl_3} = 6.3 \times 10^{-3}$ m).

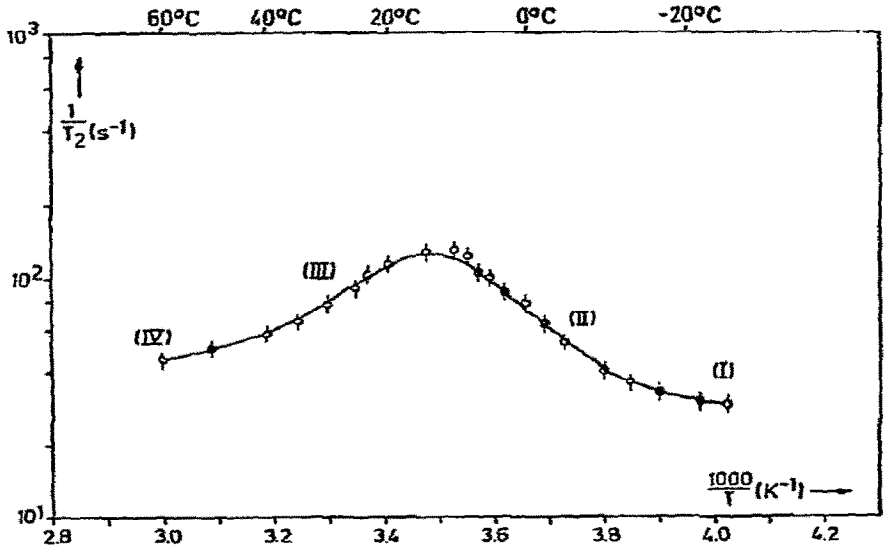

Fig. 2. Spin–spin relaxation rate of the α protons of bulk phase pyridine in solutions of Fe(III)–PPD in $C_5H_5N/CDCl_3$ at various temperatures ($C_M = 2.7 \times 10^{-5}$ m; $C_A = 6.2 \times 10^{-4}$ m; $C_{CDCl_3} = 5.5 \times 10^{-3}$ m).

experimental NMR line widths ($\Delta\nu = 1/T_2\pi$) of the α protons in the bulk phase of pyridine in solutions of Fe(II)– or Fe(III)–PPD in $CDCl_3/C_5H_5N$ are presented in a semilogarithmic plot [log (T_2^{-1}) versus reciprocal temperature] in figs. 1 and 2. In fig. 3 the corresponding chemical shifts are shown. The devia-

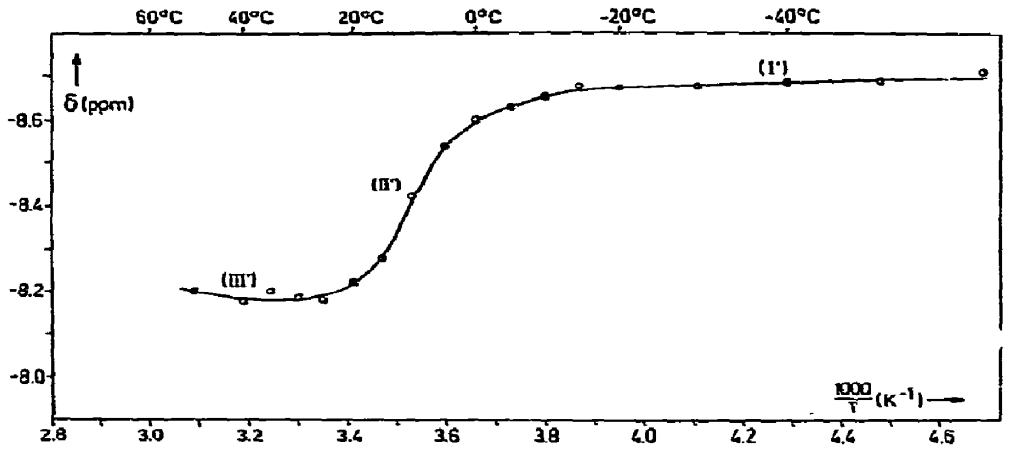

Fig. 3. Chemical shift of the α protons of bulk phase pyridine at various temperatures in solutions of Fe(II)–PPD in $C_5H_5N/CDCl_3$.

Table 1
Chemical shifts δ and spin–spin relaxation times T_2 of α and β protons for coordinated (M) and non-coordinated (A) pyridine at 253 K

	δ_α^A (ppm)	δ_β^A (ppm)	δ_α^M (ppm)	δ_β^M (ppm)	T_2^A (msec)	T_2^M (msec)
Fe(II)–PPD	–8.67	–7.32	– 1.27	– 4.7	≈ 30	≈ 25
Fe(III)–PPD	–8.67	–7.32	+10.5	–17	≈ 34	< 5

tions from linearity of log (T_2^{-1}) with a maximum at about 283 K immediately demonstrate the chemical exchange between coordinated and non-coordinated pyridine. At temperatures $T \leqslant 253$ K separate NMR signals appear for the coordinated protons (region I and I' in figs. 1–3). The chemical shifts and spin–spin relaxation times for the α and β protons of coordinated and non-coordinated PY at 253 K are listed in table 1. To derive the concentration of coordinated species their coordination number is needed. It was obtained by a comparison of the area under the PY absorption signals with the intensity of, for example, the methyl protons from Fe–PPD yielding a pyridine coordination number, $n = 2$.

Following the approach described by Hahn and Maxwell [11], and McConnell [12] the changes of line width and chemical shift caused by jumps of nuclei from site A (bulk phase) to site M (coordination sphere) may be obtained by rigorous solution of the corresponding Bloch equation. For a system, as the one under consideration, in which the metal ion is highly diluted, i.e., the concentration of non-coordinated species c_A is much higher than the concentration c_M of coordinated molecules, $c_A \gg c_M$, the relaxation time is given [13] by:

$$1/T_2 - 1/T_{2A} = (x_M/\tau_M) \times [T_{2M}^{-2} + (T_{2M}\tau_M)^{-1} + \Delta\omega_M^2]/[(T_{2M}^{-1} + \tau_M^{-1})^2 + \Delta\omega_M^2], \quad (1)$$

where T_2 is the observed relaxation time, T_{2A} corresponds to the line width of the nuclei in environment A (bulk phase), T_{2M} describes the magnetic relaxation which the coordinated nuclei experience, $\Delta\omega_M$ stands for the difference of Larmor frequencies between the coordinated and non-coordinated nuclei and x_M gives the molar ratio of coordinated species. Finally, τ_M symbolizes the mean lifetime of the considered species in the coordination sphere of the metal porphyrin.

In analogy to eq. (1) the frequency shift of solvent (A) due to chemical exchange is given [13] by:

$$\Delta\omega_p = -(\Delta\omega_M/\tau_A\tau_M)[(1/T_{2M} + 1/\tau_M)^2 + \Delta\omega_M^2]^{-1}, \quad (2)$$

where $\Delta\omega_p$ is the experimental resonance frequency minus that of the pure solvent (A). τ_A gives the mean lifetime of nuclei in the bulk phase. From $x_A \gg x_M$ follows $\tau_A \gg \tau_M$. It is convenient to consider the implications of eqs. (1) and (2) for certain limiting cases depending on the magnitude of τ_M:

(a) $\Delta\omega_M^2 \gg T_{2M}^{-2}, \tau_M^{-2}$;

$$1/T_2 - 1/T_{2A} = x_M/\tau_M; \quad (1a)$$

$$\Delta\omega_p = -x_M \Delta\omega_M^{-1} \tau_M^{-2}. \quad (2a)$$

(b) $T_{2M}^{-2} \gg \Delta\omega_M^2, \tau_M^{-2}$;

$$1/T_2 - 1/T_{2A} = x_M/\tau_M; \quad (1b)$$

$$\Delta\omega_p = -x_M \Delta\omega_M T_{2M}^2 \tau_M^{-2}. \quad (2b)$$

The results obtained under (a) and (b) are valid for slow exchange. The regions for which eqs. (1a, b) and (2a, b) hold, are indicated by II and II′ in figs. 1–3. If, on the other hand, the exchange rate is rapid, the line width and frequency changes with temperature as shown in figs. 1–3 (region III, III′ and IV). As before, there are two possibilities:

(c) $\tau_M^{-2} \gg \Delta\omega_M^2 \gg (T_{2M}\tau_M)^{-1}$,

$$1/T_2 - 1/T_{2A} = x_M \tau_M \Delta\omega_M^2; \quad (1c)$$

$$\Delta\omega_p = -x_M \Delta\omega_M. \quad (2c)$$

(d) $(T_{2M}\tau_M)^{-1} \gg T_{2M}^{-2}, \Delta\omega_M^2$;

$$1/T_2 - 1/T_{2A} = x_M/T_{2M}; \quad (1d)$$

$$\Delta\omega_p = -x_M \Delta\omega_M. \quad (2d)$$

The kinetic parameters, τ_M, $\Delta H^{\neq}$, and $\Delta S^{\neq}$ which are collected in table 2 were determined by fitting the data in figs. 1–3 to eqs. (1a–d) and (2a–d), using a non-linear least squares computer program. The temperature dependence of τ_M was taken as:

$$\tau_M = (h/kT) \exp [\Delta H^{\neq}/RT - \Delta S^{\neq}/R]. \quad (3)$$

In the present case τ_M has to be considered as a weighted average for PY in the coordination sphere of low- and high-spin Fe–PPD (cf. fig. 4) and may be defined as

$$1/\tau_M = x_L 1/\tau_L + x_H 1/\tau_H, \quad (4)$$

with the mole ratios x_L, x_H of species in low- and high-spin state and the corresponding exchange rates, τ_L^{-1}, τ_H^{-1}. Exchange of PY between low- and high-spin Fe–PPD is too slow to contribute essentially to τ_M, as will be seen below.

The transition of Fe–PPD form a low-spin towards a high-spin electron configuration with increasing temperature is demonstrated in fig. 4. The effective magnetic moment μ_{eff} [Fe(II)–PPD] $\approx 0\ \mu_B$ and μ_{eff} [Fe(III)–PPD] $\approx 2.4\ \mu_B$ at temperatures below 253 K indicates that the bis-pyridine complexes of both species are in the low-spin electron state. The somewhat higher value for Fe(III)–PPD than those expected for a pure spin moment with $S = \frac{1}{2}$ ($\mu_S = 1.73\ \mu_B$) is attributed to the existence of spin–orbit coupling resulting in an anisotropic g tensor [14]. Using the values of $\mu_{eff} = 2.4\ \mu_B$ and $\mu_{eff} = 5.92\ \mu_B$ for Fe(III)–PPD in its low- and high-spin states and the corresponding values of $\mu_{eff} = 0\ \mu_B$ and $\mu_{eff} = 4.9\ \mu_B$ for Fe(II)–PPD; the equilibrium constant between both spin states can be calculated and from its temperature dependence the following values of ΔH and ΔS, the equilibrium enthalpy and entropy are obtained:

$[\text{Fe(III)–PPD}]_L \rightleftharpoons [\text{Fe(III)–PPD}]_H$:

ΔH (298 K) = (80 ± 15) kJ · mol^{-1},

ΔS (298 K) = (280 ± 60) J · mol^{-1} K^{-1},

and

$[\text{Fe(II)–PPD}]_L \rightleftharpoons [\text{Fe(II)–PPD}]_H$:

ΔH = (25 ± 5) kJ · mol^{-1},

ΔS = (67 ± 15) J · mol^{-1} K^{-1}.

Table 2
Kinetic and thermodynamic parameters for the exchange of pyridine from bis-pyridine–Fe–PPD into the bulk solution

	τ_M(298 K) [sec]	τ_M(273 K) [sec]	$\Delta H^{\neq}$(273 K) [kJ · mol^{-1}]	$\Delta S^{\neq}$(273 K) [J · mol^{-1} K^{-1}]
Fe(II)–PPD	$(6 \pm 2) \times 10^{-5}$	$(1 \pm 0.3) \times 10^{-3}$	67 ± 7	+42 ± 4
Fe(III)–PPD	$(7 \pm 2) \times 10^{-5}$	$(0.6 \pm 0.2) \times 10^{-3}$	35.6 ± 4	−53 ± 5

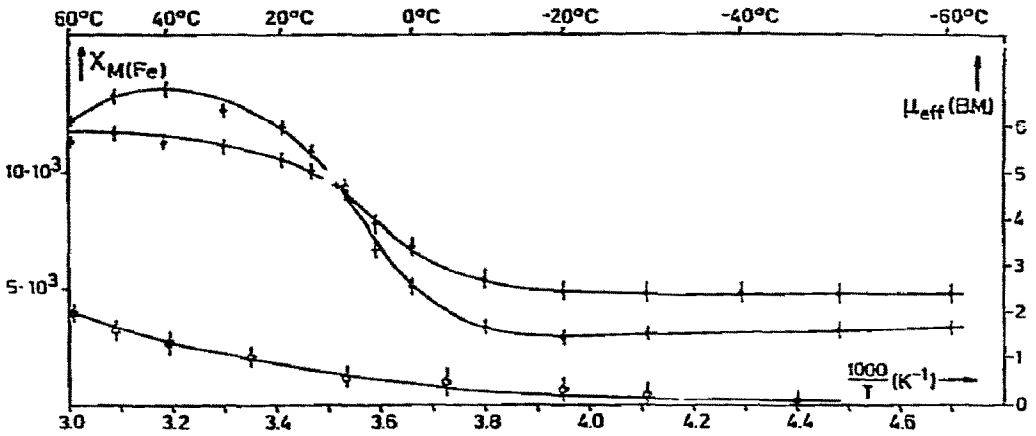

Fig. 4. Molar susceptibility χ_M and effective magnetic moment μ_{eff} of iron in Fe–PPD–$C_5H_5N/CDCl_3$ at various temperatures. For diamagnetic contributions to χ the values given in [17] have been used.
+ χ_M of Fe(III)–PPD in $C_5H_5N/CDCl_3$ (left scale), • μ_{eff} of Fe(III)–PPD in $C_5H_5N/CDCl_3$ (right scale),
○ μ_{eff} of Fe(II)–PPD in $C_5H_5N/CDCl_3$ (right scale).

The transition from low- to high-spin electron configuration for both species is accompanied by an increase of ΔS, which is higher for Fe(III)–PPD.

In fig. 5 the spin–spin relaxation rate of a methyl group fixed on the porphyrin ring of Fe(III)–PPD is represented in a semi-logarithmic plot versus T^{-1}. Again, the deviation from linearity indicates an exchange reaction with an overall relaxation rate (in the limit of slow exchange) [15] of:

$$(1/T_2)' = 1/T_2 + 1/\tau_L \qquad (5)$$

where $1/T_2$ is the relaxation rate of nuclei not experiencing an exchange reaction and τ_L gives the mean lifetime of nuclei in a particular state, i.e., the low-spin electron configuration of the metal porphyrin. Anal-

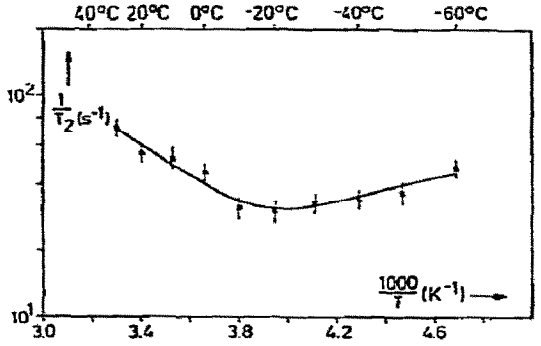

Fig. 5. Spin–spin relaxation rate of a methyl group of Fe(III)–PPD.

ysis of measured values $(1/T_2)'$ yields a mean lifetime τ_L for the methyl protons of Fe(III)–PPD in the low-spin configuration:

$$\tau_L\ (298\ \mathrm{K}) = (20 \pm 15)\ \mathrm{msec}\ .$$

From the temperature dependence the following activation parameters result:

$$\Delta H^{\neq}_{L\to H}\ (298\ \mathrm{K}) = (26 \pm 5)\ \mathrm{kJ \cdot mol^{-1}},$$

$$\Delta S^{\neq}_{L\to H}\ (298\ \mathrm{K}) = (-125 \pm 25)\ \mathrm{J \cdot mol^{-1} K^{-1}}\ .$$

Comparison between the negative value of $\Delta S^{\neq}_{L\to H}$ and the total entropy change for the low/high spin transition implies that the transition from the activated state into the high-spin configuration is accompanied by a very large increase of entropy.

Parallel to the spin transition in Fe–PPD the exchange rate of PY from the first coordination sphere into the bulk phase increases with rising temperatures. The negative value of $\Delta S^{\neq}$ and the relative small value of $\Delta H^{\neq}$ (cf. table 2) indicate that an SN2 mechanism predominates for the exchange rates of PY from the bis-pyridine Fe(III)–PPD complex. The formation of a hepta-coordinated activated complex is connected with negative values for the entropy of activation [16]. Conversely, the higher value of $\Delta H^{\neq}$ and the positive entropy of activation $\Delta S^{\neq}$ for the PY exchange from bis-pyridine Fe(II)–PPD into the bulk solvent phase seems to indicate an SN1 mechanism with a penta-

coordinated activated species. An estimate, using a simplified electrostatic model, shows that for a d^6 (low-spin) electron configuration, as it prevails for Fe(II)–PPD at low temperatures, a penta-coordinated activation complex should be more favourable energetically than its hepta-coordinated analogue [16]. With a crystal field parameter Dq of about 0.2 eV, a value which is typical of the ligand field strength, an activation energy E_a of about 75 kJ·mol^{-1} for an SN1 mechanism is expected (cf. table 2), whereas for an SN2 mechanism the activation energy would be about twice as high. Although the values for τ_M reported here give an average mean lifetime of PY in the coordination sphere of low- and high-spin Fe–PPD, the different experimental results for PY exchange rates depending on the oxidation state of Fe, may be rationalized on this very simplified electrostatic model.

4. Conclusions

The cross-over point for the low/high spin transition of bis-pyridine Fe–PPD in both oxidation states occurs close to room temperature. Parallel to this transition the rate of ligand exchange from the fifth and sixth positions of bis-pyridine Fe–PPD is accelerated. The thermodynamic equilibrium between the two spin states of Fe(III)–PPD is shifted towards the high-spin component ($\Delta G < 0$) for temperatures $T \gtrsim 280$ K, whereas for Fe(II)–PPD the values of ΔG are still positive at 333 K, indicating that the low-spin configuration of reduced Fe–PPD is the more stable species at room temperature.

Acknowledgement

We wish to thank Mr. K. Schindler for his skill and patience in preparing the various compounds.

References

[1] E. Antonini and M. Brunori, Hemoglobin and Myoglobin in their Reaction with Ligands (North-Holland, Amsterdam, 1971).
[2] G.A. Webb, in: Ann. Reports on NMR-Spectroscopy, ed. E.F. Mooney, vol. 3 (Academic Press, N.Y., 1970) p. 211.
[3] B.B. Hasinoff, H.B. Dunford and D.G. Horne, Can. J. Chem. 47 (1969) 3225.
[4] G.N. LaMar and F.A. Walker, J. Amer. Chem. Soc. 94 (1972) 8607; 90 (1973) 1662.
[5] H.A. Degani and D. Fiat, J. Amer. Chem. Soc. 93 (1971) 4281.
[6] W.S. Caughey, C.H. Barlow, D.H. O'Keeffe and M.C. O'Toole, Ann. N.Y. Acad. Sci. 206 (1973) 296.
[7] H.A.O. Hill and K.G. Morallee, J. Amer. Chem. Soc. 94 (1972) 731.
[8] D.F. Evans, Proc. Chem. Soc. (1959) 2003.
[9] J.L. Deutsch and S.M. Poling, J. Chem. Educ. 46 (1969) 167.
[10] J.E. Falk, Porphyrins and Metalloporphyrins (Elsevier, Amsterdam, 1964).
[11] E.L. Hahn and D.E. Maxwell, Phys. Rev. 88 (1952) 1070.
[12] H.M. McConnell, J. Chem. Phys. 28 (1958) 430.
[13] T.J. Swift and R. Connick, J. Chem. Phys. 37 (1962) 307.
[14] A. Daniels, E. v. Goldammer and H. Zorn, J. Eur. Bioch. (1975), in press.
[15] J.A. Pople, W.G. Schneider and H.J. Bernstein, High-Resolution NMR (McGraw-Hill, N.Y., 1959).
[16] F. Basolo and R.G. Pearson, Mechanisms of Inorganic Reactions (Wiley, N.Y., 1967) p. 124.
[17] R. Havemann, W. Haberditzl and K.H. Mader, Z. Phys. Chem. 218 (1961) 71.